Canonical Ensemble of Initial States Leading to Chiral Fluctuations

Dénes Molnár

Physics Department, University of Bergen
N-5007 Bergen, Allégaten 55, and
Physics Department, Columbia University
New York, NY 10027, USA

László P. Csernai

Physics Department, University of Bergen
N-5007 Bergen, Allégaten 55, Norway

and

Zsolt I. Lázár

Physics Department, University of Bergen
N-5007 Bergen, Allégaten 55, Norway

Final revision June 24, 1998

Abstract

In energetic heavy ion collisions, if quark-gluon plasma is formed, its hadronization may lead to observable critical fluctuations, i.e., DCC formation. The strength and observability of these fluctuations depend on the initial state. Here we study the canonical ensemble of initial states of chiral fluctuations in heavy ion collisions and the probability to obtain observable domains of chiral condensates.

PACS number(s): 12.39.Fe, 12.38.Mh, 25.75.-q

I. INTRODUCTION

In a recent article the initial states of Disoriented Chiral Condensate (DCC) were studied, the importance of non-vanishing chiral 'angular momentum' was pointed out, and the microcanonical ensemble of initial states were evaluated for fixed energy and chiral angular momentum [1]. These results indicated that the observability of DCC formation is a delicate problem, and it strongly depends on the reaction mechanism of heavy ion collisions.

Since at this moment reaction models which would predict a chiral angle distribution at the onset of hadronization do not exist, we assume that thermal equilibrium is reached in the supercooled plasma at the freeze-out, $T_{FO} = T_0 < T_c$, which coincides with the beginning of the process of hadronization [2,3]. Consequently we also assume that at this moment the chiral degrees of freedom in the system are thermalized and thus can be characterized by a canonical distribution corresponding to the freeze-out temperature, T_0, and to the volume of the system, V. (This latter quantity is vital because we study fluctuations in a small, finite system!) Unless further constraints on the chiral degrees of freedom can be established from more detailed reaction models the generated canonical distribution of chiral initial states will represent the statistical distribution in heavy ion experiments.

Having obtained this distribution we will analyze which initial configurations lead to strongly fluctuating domains of DCC, and what are the overall chances to detect these experimentally.

For our studies, just like ref. [1], we have chosen the linear sigma model because it contains the relevant chiral degrees of freedom and it is still relatively simple.

II. THE LINEAR SIGMA MODEL

The linear sigma model involves the isodoublet of the light quark fields, Ψ, and a real, four-component chiral field, $\Phi \equiv (\sigma, \vec{\pi})$, where σ is a scalar field, while $\vec{\pi} \equiv (\pi_1, \pi_2, \pi_3)$ is a triplet of pseudoscalar pions. The Lagrangian density is *

$$\mathcal{L} = \bar{\Psi}\left[i\gamma_\mu \partial^\mu - g\left(\sigma + i\gamma_5 \vec{\tau}\vec{\pi}\right)\right]\Psi + \frac{1}{2}\left(\partial_\mu \sigma\right)\left(\partial^\mu \sigma\right) + \frac{1}{2}\left(\partial_\mu \vec{\pi}\right)\left(\partial^\mu \vec{\pi}\right) - U\left(\sigma, \vec{\pi}\right) \ , \qquad (1)$$

with the so-called "Mexican hat" potential energy density

$$U\left(\sigma, \vec{\pi}\right) = \frac{\lambda}{4}\left(\sigma^2 + \vec{\pi}^2 - v^2 + \frac{T^2}{2}\right)^2 - H\sigma + U_0(T) \ , \qquad (2)$$

where the last term, $U_0(T)$, ensures that the *absolute* minimum of the potential energy density is 0. Without the $H\sigma$ term, this Lagrangian density is invariant under the chiral $SU_L(2) \otimes SU_R(2)$ transformations.

The parameters in this Lagrangian are chosen in such a way [3] that in *normal vacuum* at $T = 0$ chiral symmetry is spontaneously broken and the expectation values of the meson fields are

$$\langle\sigma\rangle = f_\pi, \quad \langle\vec{\pi}\rangle = 0 \ , \qquad (3)$$

where f_π=93 MeV is the pion decay constant. In the vacuum with broken chiral symmetry pions represent soft "azimuthal" excitations of the chiral field. To have the correct pion mass in vacuum ($T = 0$), m_π=138 MeV, one should take

*We shall use $\hbar = c = k = 1$ units.

$$v^2 = f_\pi^2 - \frac{m_\pi^2}{\lambda}, \qquad H = f_\pi m_\pi^2 \ . \tag{4}$$

The parameter λ is related to the sigma mass, $m_\sigma^2 = 2\lambda f_\pi^2 + m_\pi^2$, which can be chosen to be about 600MeV (then $\lambda \approx 20$). Sigmas represent stiff, "radial" excitations of the chiral field. The remaining coupling constant g can be fixed by the requirement that the effective quark mass, $m_q^2 = g^2(\sigma^2 + \vec{\pi}^2)$, in broken vacuum coincides with the constituent quark mass in hadrons, which is about 1/3 of the nucleon mass, m_N. This gives $g \approx (m_N/3)/f_\pi = 3.36$.

III. IDEAL HYDRODYNAMICS IN THE LOCAL REST FRAME

When solving the equations of motion corresponding to our Lagrangian (1) we shall assume a one-dimensional Bjorken scenario [4]. Consequently, we shall only consider field evolutions having one-dimensional scaling property and we shall work in the corresponding local rest (LR) frame. Therefore, let us briefly review here the properties of a scaling hydrodynamical expansion in the LR frame.

A. Framework: the Bjorken model

The local rest frame is a curvilinear coordinate system where the matter is at rest. For a longitudinal scaling expansion along the z-axis the LR frame coordinates, $x^i \equiv (\tau, x, y, \eta)$, are given by the c.m. coordinates, $x^\mu \equiv (t, x, y, z)$, as

$$\tau \equiv \sqrt{t^2 - z^2} \qquad \text{and} \qquad \eta \equiv \frac{1}{2}\ln\frac{t+z}{t-z}. \tag{5}$$

Thus, the invariant space-time interval in the LR frame is $ds = d\tau^2 - dx^2 - dy^2 - \tau^2 d\eta^2$, therefore the covariant metric tensor is

$$g_{ik} = \mathrm{diag}(1, -1, -1, -\tau^2). \tag{6}$$

This metric tensor gives rise to three non-vanishing Christoffel symbols: $\Gamma^0_{33} = \tau$, $\Gamma^3_{30} = \Gamma^3_{03} = 1/\tau$.
The equations of ideal hydrodynamics are the conservation laws given by the requirement that the energy momentum tensor, T_i^k, has a vanishing divergence, i.e., $T^k_{i;k} = 0$. [5] Expressing this divergence in terms of the partial derivatives and the Christoffel symbols, we arrive to the following four equations:

$$T^k_{0;k} = \frac{\partial T^k_0}{\partial x^k} + \frac{1}{\tau}\left(T^0_0 - T^3_3\right) \ , \qquad T^k_{1;k} = \frac{\partial T^k_1}{\partial x^k} + \frac{1}{\tau}T^0_1 \ ,$$
$$T^k_{2;k} = \frac{\partial T^k_2}{\partial x^k} + \frac{1}{\tau}T^0_2 \ , \qquad T^k_{3;k} = \frac{\partial T^k_3}{\partial x^k} - \tau T^3_0 \ . \tag{7}$$

In local thermal equilibrium, if we neglect the effects of viscosity and heat conductivity, the energy momentum tensor has the form [6] $T_{ik} = (e+p)\,u_i u_k - p\,g_{ik}$, where e is the energy density, p is the pressure in the co-moving frame, and u_i is the flow velocity of the matter. Thus, in the LR frame the energy momentum tensor is diagonal, i.e.,

$$T_i^k = \mathrm{diag}\,(e, -p, -p, -p)\,. \tag{8}$$

The conservation laws (7) lead to

$$\frac{\partial e}{\partial \tau} + \frac{p+e}{\tau} = 0, \qquad \frac{\partial p}{\partial x} = \frac{\partial p}{\partial y} = \frac{\partial p}{\partial \eta} = 0. \tag{9}$$

These, together with the charge conservations

$$D_i\left(\rho_c u^i\right) = 0,$$

(where c runs for all conserved charges, and D_i stands for the covariant derivative) and the equation of state (EoS) which connects the pressure, energy density, and the *proper* charge densities ρ_c [$\rho_c \equiv dN_c/(dx\,dy\,d\eta)$], form a closed set of equations, which can be solved for given initial and boundary conditions. In the LR frame the charge conservations simplify to

$$\frac{\partial \rho_c}{\partial \tau} = 0. \tag{10}$$

The equation of the Bjorken model can be obtained by imposing the boost invariance and transverse translational invariance of e, p and ρ_c. Then, by Eqs. (10), the charges are constants of motion: $\rho_c(\tau) = \rho_c(\tau_0)$. Eqs. (9) simplify to an initial value problem for an ordinary differential equation in τ:

$$\frac{de(\tau)}{d\tau} + \frac{p(\tau) + e(\tau)}{\tau} = 0, \tag{11}$$

with $e(\tau_0) = e_0$, where $p = p(e, \rho_{c0})$ is given by the EoS.

B. Scaling expansion in the linear sigma model

Let us consider the sigma model without quarks ($g = 0$). Then the Lagrangian density (1), in a general curvilinear coordinate system, is

$$\mathcal{L} = \frac{1}{2}\left(\partial_i \Phi_r\right) g^{ik} \left(\partial_k \Phi_r\right) - U(\Phi_r, T), \tag{12}$$

where $\partial_i \equiv \frac{\partial}{\partial x^i}$, $\Phi_r = (\sigma, \vec{\pi})$, there is an implied summation for indices occurring twice (i, k and r), and

$$U(\sigma, \vec{\pi}, T) = \frac{\lambda}{4}\left(\sigma^2 + \vec{\pi}^2 - v^2 + \frac{1}{2}T^2(x^i)\right)^2 - H\sigma + U_0,$$

where x^i is a space-time coordinate $x^i = (\tau, x, y, \eta)$.

The energy-momentum tensor, T_{ik}, can be obtained from the Lagrangian density using the relation[†] [5]

$$-\frac{1}{2}\sqrt{-g}\,T_{ik} = \frac{\partial}{\partial x^l}\frac{\partial\sqrt{-g}\,\mathcal{L}}{\partial\frac{\partial g^{ik}}{\partial x^l}} - \frac{\partial\sqrt{-g}\,\mathcal{L}}{\partial g^{ik}},$$

where g stands for the determinant of the metric tensor, g_{ik}. A straightforward calculation gives

$$T_{ik} = (\partial_i\Phi_r)\,(\partial_k\Phi_r) - \mathcal{L}\,g_{ik}. \tag{13}$$

This is, unlike the energy-momentum tensor in the Bjorken model, generally not diagonal. However, if we impose boost invariance, the off-diagonal elements in the energy-momentum tensor vanish. From Eqs. (13), (12) and (6), we can easily obtain the diagonal elements:

$$\begin{aligned} T_0^0 &= \frac{1}{2}\,(\partial_\tau\Phi_r)\,(\partial_\tau\Phi_r) + U(\Phi_r) \equiv e_{kin} + e_{pot} \equiv e \\ T_1^1 &= \frac{1}{2}\,(\partial_\tau\Phi_r)\,(\partial_\tau\Phi_r) - U(\Phi_r) \equiv e_{kin} - e_{pot} \equiv -p \\ T_2^2 &= T_3^3 = T_1^1, \end{aligned} \tag{14}$$

where $e_{kin} \equiv \frac{1}{2}\,(\partial_\tau\Phi_r)\,(\partial_\tau\Phi_r)$ is the kinetic energy density and $e_{pot} \equiv U$ is the potential energy density, and we introduced the total energy density, $e \equiv e_{kin} + e_{pot}$, and $p \equiv e_{pot} - e_{kin}$. These are functions of the proper time τ as the fields follow the equations of motion (EoM).
Obviously, the energy momentum tensor now has the form (8), therefore the conservation laws (9) and all their consequences are also valid now. Particularly, this leads to

$$\frac{de}{d\tau} = -\frac{e+p}{\tau} = -2\frac{e_{kin}}{\tau}\ , \tag{15}$$

which can be seen as a generalization of the usual energy conservation for our expanding system. We used this equation as a check of the numerical solution of the equations of motion.
To obtain how the *total* energy evolves, we have to take the expansion into account. The surface element of the $\tau = const.$ hyperplane is $d\Sigma = \tau d\eta\, dx\, dy$. Therefore, the volume of our longitudinally expanding system is proportional to τ, i.e., $dV/d\tau = V/\tau$. Now, with the help of the conservation laws (11), the time derivative of the total energy, $E \equiv Ve$, can be expressed as

$$\frac{dE}{d\tau} = \frac{E_{pot} - E_{kin}}{\tau} = -p\,\frac{dV}{d\tau}\ , \tag{16}$$

where $E_{kin} \equiv V\,e_{kin}$ is the kinetic energy and $E_{pot} \equiv V\,e_{pot}$ is the potential energy of our expanding system. The interpretation of Eq. (16) could be similar to that of the corresponding equation for the Bjorken model, Eq. (11). However, for the sigma model we can easily have a negative pressure, which corresponds to an *increase* of the total energy during expansion! This is the case if $E_{pot} > E_{kin}$ in Eq. (16), which is typical for the early evolution in the quench scenario. We also note that, as pointed out already in ref. [4], Eq. (16) means that we have an isentropic (adiabatic) expansion.

[†]Our sign convention in the space-time interval is different from that of ref. [5]; therefore, we have a *minus* sign on the left hand side.

IV. EQUATIONS OF MOTION

In the mean-field approximation, ignoring all-loop contributions and considering σ and $\vec{\pi}$ as classical fields, we can obtain the following equations motion [7,8,3] :

$$\begin{aligned} \partial_\mu\partial^\mu\sigma(x) + \lambda\left[\sigma^2(x)+\vec{\pi}^2(x)-v'^2(x)\right]\sigma(x) &\\ -H = -g\rho_S(x), &\\ \partial_\mu\partial^\mu\vec{\pi}(x) + \lambda\left[\sigma^2(x)+\vec{\pi}^2(x)-v'^2(x)\right]\vec{\pi}(x) = -g\vec{\rho}_P(x), & \end{aligned} \tag{17}$$

where $v'^2(x) \equiv v^2 - T^2(x)/2$. Here $\rho_S \equiv \langle\bar{q}q\rangle$ and $\vec{\rho}_P \equiv i\langle\bar{q}\gamma_5\vec{\tau}q\rangle$ are the scalar and pseudoscalar quark densities, which should be determined self-consistently from the motion of q and $\bar{q}$ in the background meson fields. The scalar and pseudoscalar densities can be represented as [3]

$$\rho_S(x) = ga(x)\sigma(x), \quad \vec{\rho}_P(x) = ga(x)\vec{\pi}(x), \tag{18}$$

where $a(x)$ is expressed in terms of the momentum distribution of quarks and antiquarks $f(x,p)$:

$$\begin{aligned} a(x) &= \nu_q\int\frac{d^4p}{(2\pi\hbar)^3}\ 2\delta(p^\mu p_\mu - m^2(x))f(x,p) \\ &\longrightarrow \frac{\nu_q}{(2\pi\hbar)^3}\int\frac{d^3p}{E(x,\mathbf{p})}[n_q(x,\mathbf{p}) + n_{\bar{q}}(x,\mathbf{p})]\ . \end{aligned} \tag{19}$$

Here ν_q is the degeneracy factor of quarks which equals to 12 in our case (flavour × spin × colour).
Let us consider a one-dimensional Bjorken scaling and assume that the quark distribution is an ideal Fermi distribution at the freeze-out time τ_0 (following [2,3] we can take $\tau_0 \sim 7\mathrm{fm}/c$) while the subsequent distribution for time $\tau > \tau_0$ is given by the solution of the collisionless Vlasov equation [3]. Then the source term, $a(x)$, can be cast into [9]:

$$\begin{aligned} a(x) \equiv a(\tau) = &\frac{\nu_q\alpha}{\pi^2\sqrt{1-\alpha^2}}\ T_0^2 \\ &\times\int_0^\infty dq\ q\ \frac{\arcsin\sqrt{(1-\alpha^2)\,/\left(\frac{m^2(\tau)}{T_0^2q^2}+1\right)}}{\exp\left(\sqrt{q^2+m^2(\tau_0)/T_0^2}-\frac{\mu_0}{T_0}\right)+1}\ , \end{aligned}$$

where $\alpha \equiv \tau_0/\tau$, T_0 and μ_0 are the freeze-out temperature and chemical potential. For the $\mu_0 = 0$, $m_q = 0$ case

this expression can be integrated analytically [3], while in the general $m_q \neq 0$, $\mu_0 \neq 0$ case it can be evaluated numerically using an eight-point Gauss–Laguerre integral formula [9]. This way we can follow the solution of the EoM numerically from an arbitrary initial condition at τ_0 during the whole symmetry breaking process. For simplicity, we shall assume that quarks and antiquarks are in chemical equilibrium, i.e., we take $\mu_0 = 0$.

To solve the EoM, we need to know the temperature field, $T(x)$. However, following [10,11] we may assume that the cooling is very fast and then we may take $T(x) \equiv 0$. This is the so-called *quench* scenario. Certainly, the quench is an idealization since in a real collision thermal fluctuations will not cease instantaneously. Now the EoM has no reference to any temperature but the initial condition, which we choose to be at the freeze-out of the quarks, must represent the freeze-out temperature, $T_0 \approx 130 - 140$MeV. We emphasize that our scenario differs from the original quench because, even though the thermal fluctuations of the fields are neglected, we still have an interaction with the expanding quark/antiquark background. One could choose other possible non-equilibrium scenarios, for example, *annealing* [12,13].

Before the quench, the system can typically be found somewhere around the minimum of the potential energy density. However, when the quench occurs, the position of this minimum suddenly changes to the physical vacuum, $(\sigma, \vec{\pi}) = (f_\pi, \vec{0})$. Thus, the system finds itself on the slope of the "valley" of the potential, rolls down towards its new minimum, and oscillates around it [8,14,15,9]. The oscillations are damped because, due to the expansion, there is a first order derivative in the EoM (17), therefore the fields finally relax to the physical vacuum, $(f_\pi, \vec{0})$.

Studies show [15,9] that the main effect of the quarks is an additional damping; the oscillations of the chiral fields are reduced by about $40 - 50\%$. This is due to the fact that during the transition a portion of the energy of the system is used up for the increasing quark mass. Also, the phase transition happens about 0.5fm/c slower; it takes about 2.5fm/c. The presence of quarks has a strong influence on the onset of instabilities and domain formation in the initially homogeneous system. This we shall address in a separate paper.

V. THE QUESTION OF THE INITIAL CONDITION

The physical choice of initial condition or ensembles of initial states was not studied in detail in earlier works, although this is a vital problem if we want to predict the observability of DCC fluctuations. An early study [14] followed by refs. [15,9] assumed the initial condition:

$$\sigma_0 = 0,\ \vec{\pi}_0 = \vec{0},$$
$$\dot{\sigma_0} = 1\text{MeV}\, c/\text{fm},\ \dot{\vec{\pi}}_0 = (5,0,0)\text{MeV}\, c/\text{fm}, \qquad (20)$$

with $\tau_0 = 1$fm/c. This choice of the chiral field configuration corresponds to the chirally symmetric phase representing very hot quark-gluon plasma, i.e., when $H = 0$ and $T > T_c = \sqrt{2}v$ (≈ 124MeV). The initial value of the fields was assumed to be the value of the condensate, which is zero in this case, i.e., $\langle\sigma\rangle = 0$ and $\langle\vec{\pi}\rangle = 0$.

However, to get the correct value of the pion mass in the physical vacuum, we do need the explicit symmetry breaking term $H\sigma$. Hence, in the minimum of the potential the condensate is never zero, though it gets close to zero for temperatures above $250 - 300$MeV (see Fig. 1). However, at the freeze-out temperature, $T_0 = 130$MeV, we have a large condensate of 40MeV.

Another important factor is that our system is finite, therefore thermal fluctuations are of real importance. Due to the fluctuations, the system is at the minimum of the potential energy density only *on the average*, and the probability for finding it somewhere around this minimum can be considerable, especially for very small systems and/or high temperatures. Therefore, the time evolution starting from the minimum of the potential energy density is not fully representative for the majority of the realistic initial states.

Furthermore, the system has a considerable kinetic energy at the temperatures under consideration. This should be reflected by the choice of the initial value of the field derivatives. Our analysis will show that the initial condition (20) has too little kinetic energy for the temperatures we are considering, even if we go down to as low as $T = 130$MeV. Thus, the picture of a system on the "top" of the potential started with a little "kick" cannot be realistic.

These considerations lead us to propose an initial condition, which is closer to the physical picture we have at the time of the freeze-out. Before the freeze-out the system can be approximated to be in thermal equilibrium at a given temperature, T, and it has a given volume, V. If so, then the initial condition should be chosen according to a canonical thermal ensemble, i.e., the probability p of a configuration $(\sigma, \vec{\pi}, \dot{\sigma}, \dot{\vec{\pi}})$ is proportional to the Boltzmann-factor, P:

$$p(\sigma, \vec{\pi}, \dot{\sigma}, \dot{\vec{\pi}}) \propto \exp\left[-\frac{V}{T}\mathcal{H}(\sigma, \vec{\pi}, \dot{\sigma}, \dot{\vec{\pi}})\right] \equiv P(\sigma, \vec{\pi}, \dot{\sigma}, \dot{\vec{\pi}}) \qquad (21)$$

where $\mathcal{H}$ is the Hamiltonian density, the dot stands for $\partial/\partial\tau$, and we assumed that the system is homogeneous and we have taken the Bjorken scaling granted. The Hamiltonian density consists of three terms, $\mathcal{H}_{kin}$, $\mathcal{H}_{pot}$ and $\mathcal{H}_q$, which are respectively the kinetic and potential energy density of the chiral fields and the energy density of the quarks (with $\mu = 0$):

$$\mathcal{H}_q = \nu_q \int \frac{d^3p}{E}\, E^2\, [f_q(x,\vec{p}) + f_{\bar{q}}(x,\vec{p})]$$

$$= \frac{2\nu_q}{(2\pi)^3} \int d^3p \, \frac{\sqrt{\vec{p}^2+m^2}}{\exp\left[\sqrt{\vec{p}^2+m^2}/T\right]+1}$$

$$\mathcal{H}_{kin} = \frac{1}{2}\dot{\sigma}^2 + \frac{1}{2}\dot{\vec{\pi}}^2$$

$$\mathcal{H}_{pot} = U(\sigma,\vec{\pi}) = \frac{\lambda}{4}\left(\sigma^2+\vec{\pi}^2-v'^2\right)^2 - H\sigma + U_0 \ , \quad (22)$$

where the effective quark (antiquark) mass is given as $m^2 = g^2(\sigma^2+\vec{\pi}^2)$.

Similar approaches can be found in the literature where Gaussian distributions were considered [11–14]. However, as the potential energy density is not quadratic and we also have the quark term, the distribution of the chiral fields is clearly non-Gaussian. We shall give a comparison to the initial condition of refs. [11,12]:

$$\langle\phi\rangle = \langle\dot{\phi}\rangle = 0, \ \langle\phi^2\rangle = v^2/4, \ \langle\dot{\phi}^2\rangle = v^2/1\mathrm{fm}^2. \quad (23)$$

A forerunner of the present analysis is ref. [1] where we considered initial conditions with large chiral "angular momenta", I, i.e., states where the chiral fields circle around the minimum of the potential energy density having a trajectory which is far from the minimum. As we have shown there, these states as well lead to DCC formation during the fast linear expansion. However, the magnitude of I remained an open question. Now we shall extend the analysis by including the initial distribution of finite chiral 'angular momentum' states.

There are several methods to generate the ensemble of the initial conditions. In ref. [1] we needed a *microcanonical* ensemble around a specified value of the "angular momenta", I. This ensemble was obtained by sampling the time evolution of the fields evenly in the case with explicit symmetry breaking but without quarks and expansion (Fig. 2). In this case I is not a constant of motion but oscillates in a certain interval. This method is based on the assumption of the ergodicity of the system, i.e., that during the time evolution the system gets arbitrarily close to any point in the available phase space. It is also possible to generate a *canonical* ensemble based on ergodicity. In ref. [16] a Langevin type equation of motion was used to generate such initial states, where a connection to an external heatbath of a given temperature was assumed. Then, based on the ergodicity, the states at different times correspond to a canonical ensemble of the system.

In this work we generate our initial canonical ensemble using a different method, namely the Monte–Carlo method. Consequently, we shall use a different formalism from that in ref. [1] or ref. [16].

A. The generation of the canonical distribution

To generate the canonical distribution (21), we used a simple generalization of the so-called rejection method [17] for a multidimensional probability distribution on a boundless manifold. A convenience of our method is that it does not require proper normalization of the probability distribution, i.e., the evaluation of the normalization factor.

To apply the method we need to find a function, $F(\sigma,\vec{\pi},\dot{\sigma},\dot{\vec{\pi}})$, which is everywhere above $P(\sigma,\vec{\pi},\dot{\sigma},\dot{\vec{\pi}})$ and is proportional to a distribution, $f(\sigma,\vec{\pi},\dot{\sigma},\dot{\vec{\pi}})$, which we are able to generate. It is simple to prove that if one generates a (8-dimensional) random deviate, $(\sigma,\vec{\pi},\dot{\sigma},\dot{\vec{\pi}})$, of f and a uniform deviate y between 0 and $F(\sigma,\vec{\pi},\dot{\sigma},\dot{\vec{\pi}})$, then the $(\sigma,\vec{\pi},\dot{\sigma},\dot{\vec{\pi}},y)$ points will be uniform in the (9-dimensional) volume under the graph of F. If now one keeps the point $(\sigma,\vec{\pi},\dot{\sigma},\dot{\vec{\pi}},y)$ whenever it is under P and rejects it if not, the accepted $(\sigma,\vec{\pi},\dot{\sigma},\dot{\vec{\pi}})$ points will have the desired $p(\sigma,\vec{\pi},\dot{\sigma},\dot{\vec{\pi}})$ distribution. The fraction of accepted points, i.e., the efficiency of the method is

$$A = \frac{\int\cdots\int F(\sigma,\vec{\pi},\dot{\sigma},\dot{\vec{\pi}})\, d\sigma\, d^3\pi\, d\dot{\sigma}\, d^3\dot{\pi}}{\int\cdots\int P(\sigma,\vec{\pi},\dot{\sigma},\dot{\vec{\pi}})\, d\sigma\, d^3\pi\, d\dot{\sigma}\, d^3\dot{\pi}} \ .$$

To make it easy to generate the f distribution corresponding to F, we shall choose F to be proportional to a product of Gaussian deviates:

$$\begin{aligned} F(\sigma,\vec{\pi},\dot{\sigma},\dot{\vec{\pi}}) &= Ce^{-C_1(\sigma-\sigma_m)^2}e^{-C_1\vec{\pi}^2}e^{-C_2\dot{\sigma}^2}e^{-C_2\dot{\vec{\pi}}^2} \\ &\equiv F_1(\sigma,\vec{\pi})\times F_2(\dot{\sigma},\dot{\vec{\pi}}). \end{aligned} \quad (24)$$

Now f will simply factorize into one-dimensional Gaussian distributions of the chiral fields and their derivatives. These Gaussian deviates can be generated using the routine *gasdev* described in ref. [17]. The random number generator we used is the routine *ran2* in ref. [17].

1. The choice of the comparison function

We have to choose the parameters, C, C_1, C_2 and σ_m, in F such that

$$F(\sigma,\vec{\pi},\dot{\sigma},\dot{\vec{\pi}}) \le P(\sigma,\vec{\pi},\dot{\sigma},\dot{\vec{\pi}}) \quad (25)$$

for all values of the chiral fields and their derivatives.

The coefficient C_2 is determined by the kinetic energy density term because the field derivatives appear only there. Since it is a quadratic function of the derivatives, it is straightforward to choose $C_2 = V/2T$, i.e.,

$$F_2(\dot{\sigma},\dot{\vec{\pi}}) = \exp\left[-\frac{V}{2T}\left(\dot{\sigma}^2+\dot{\vec{\pi}}^2\right)\right]. \quad (26)$$

The fields are in the other two terms of the Hamiltonian density, which are not quadratic, therefore we need approximations. With the help of Eq. (26), inequality (25) can be written as

$$\frac{V}{T}\left(\mathcal{H}_{pot}+\mathcal{H}_q\right) \ge C_1\left(\sigma-\sigma_m\right)^2 + C_1\vec{\pi}^2 + const.,$$

thus we have to approximate the potential and quark energy density terms with a quadratic expression from *below*.

The quark energy density contains the fields in a rather intractable integral. It is a monotone decreasing function of the quark mass and it is in the range between 0 and 257MeV/fm^3. It turns out to be sufficient to take a simple, crude lower bound of the form $L - Mm^2$, where $M > 0$.

It is enough to deal with the quartic term in the potential energy density (22), since the remaining $H\sigma$ term can easily be combined with any quadratic expression of σ into a final $C_1\left(\sigma - \sigma_m\right)^2$ quadratic expression. The quartic term has the general form $C'\left(a^2 \pm 1\right)^2$, where $a^2 \equiv \left(\sigma^2 + \vec{\pi}^2\right)/|v'^2|$, the upper sign $(+)$ corresponds to $T > T_c$ while the lower one $(-)$ to $T < T_c$, and C' does not contain the fields. We approximate this expression by a quadratic one using that $\left(a^2 \pm 1\right)^2 \geq la^2 - k$, if

$$0 \leq l \leq 2\sqrt{k+1} \pm 2. \tag{27}$$

Putting everything together, the first part of the comparison function is

$$F_1(\sigma, \vec{\pi}) = \exp\left\{-\frac{V}{T}\frac{\lambda^2 l'|v'^2|}{4}\left[\left(\sigma - \frac{2H}{\lambda^2 l'|v'^2|}\right)^2 + \vec{\pi}^2\right]\right\} \times \exp\left[\frac{V}{T}\left(\frac{H^2}{\lambda^2 l'|v'^2|} + \frac{\lambda^2 v'^4 k}{4} - L\right)\right], \tag{28}$$

with $l' \equiv l - 4Mg^2/\lambda^2|v'^2|$.

It is crucial to choose the parameters l, k, L and M such that we have a reasonable efficiency. Clearly, to get the highest efficiency we have to minimize the area under F_1. It is easy to see that for a fixed l we need k to be minimal, thus we have to take the upper limit in Ineq. (27), $l = 2\sqrt{k+1} \pm 2$. Since the quark energy density is a convex function of m^2, for a given M the optimal, i.e., the largest L is given by the tangent line that has a slope $(-M)$. Now we have only k and M left. For a given M, the minimum condition for the area under F_1 leads to a third-order algebraic equation for k that we solved numerically. M we set by trial and error. Having the above optimization we obtained an efficiency of 30—60%.

The quark energy can be expressed as [6]

$$\mathcal{H}_q = \frac{\nu_q}{2\pi^2}Tm^2\sum_{k=1}^{\infty}(-1)^{k-1}\left[\frac{m}{k}K_3\left(\frac{km}{T}\right) - \frac{T}{k^2}K_2\left(\frac{km}{T}\right)\right],$$

where K_n stands for the modified Bessel function of the second kind of n-th order. Certainly, we cannot take into account all terms here but that is unnecessary as the sum is convergent. We summed up the terms until the relative change of the sum became less than 10^{-6} (this corresponds to $4 - 16$ terms).

The above formula cannot be used directly for $m = 0$ and for $T = 0$. For $m = 0$ we can obtain the expression [6] $\mathcal{H}_q = 7\pi^2\nu_q T^4/120$. For $T = 0$ the integrand and thus the quark energy density is zero (see ref. [6], Section 7.3).

B. An advantage of the symmetries of the Hamiltonian

Though it does not take long to generate the ensemble of the proper initial conditions, it is very time-consuming to compute the time evolution from the several thousand initial states. However, it is possible to exploit the symmetries of the Hamiltonian to reduce the computation.

It is easy to verify the following symmetry: if a trajectory $(\sigma(\tau), \vec{\pi}(\tau))$ satisfies the EoM (17), so does the trajectory $(\sigma(\tau), \mathbf{O}\vec{\pi}(\tau))$, where $\mathbf{O}$ is an arbitrary, 3×3 rotation matrix in isospin space. Obviously, the rotation implies that the initial condition as well should be rotated. Now, if we have data for a given initial condition, we at once know the results for all other initial conditions obtained from this given one by rotations; we simply have to rotate the pion fields using the same rotations.

In this sense all rotationally equivalent initial conditions are the same. We may use this to reduce the number of parameters in the initial condition. Originally these are 8 (four fields + four derivatives). However, taking into account the rotations we may fix two pion fields and the sign of the third one, e.g., we can take $\pi_1 = \pi_2 = 0$ and $\pi_3 \geq 0$, and we can also fix one derivative, e.g., $\dot{\pi}_2 = 0$. Thus, we have only 5 parameters left.

Since our canonical distribution contains the pion fields only through $\vec{\pi}^2$ and $\dot{\vec{\pi}}^2$, it is convenient to reexpress the above parametrisation using the length of the isovector, $|\vec{\pi}|$, the length of the derivative, $|\dot{\vec{\pi}}|$, and the angle, θ, between $\vec{\pi}$ and $\dot{\vec{\pi}}$. Their relation to the previously used parameters is trivial: $\pi_3 = |\vec{\pi}|$, $(\dot{\pi_3}, \dot{\pi_1}) = |\dot{\vec{\pi}}|(\cos\theta, \sin\theta)$. Now we may realize the distribution in spherical coordinates:

$$\exp\left[-\frac{V}{T}\mathcal{H}(\sigma, \vec{\pi}, \dot{\sigma}, \dot{\vec{\sigma}})\right] d\sigma\, d\vec{\pi}\, d\dot{\sigma}\, d\dot{\vec{\pi}} = \exp\left[-\frac{V}{T}\mathcal{H}(\sigma, |\vec{\pi}|, \dot{\sigma}, |\dot{\vec{\pi}}|)\right] \vec{\pi}^2\dot{\vec{\pi}}^2 d\sigma\, d|\vec{\pi}|\, d\dot{\sigma}\, d|\dot{\vec{\pi}}| \times \sin\Theta\, d\Theta\, d\Phi\, \sin\vartheta\, d\vartheta\, d\varphi\ , \tag{29}$$

where the angles ϑ and φ correspond[‡] to $\vec{\pi}$, while the other two angles, Θ and Φ, correspond to $\dot{\vec{\pi}}$. The orientation of the two spherical frames can be chosen arbitrarily. We take the choice when $\vec{\pi}$ is along the z-axis in the frame of $\dot{\vec{\pi}}$ because then Θ is the angle between these two vectors. Exploiting the rotational invariance, the angles φ, ϑ and Φ can be fixed, e.g., to $\varphi = \vartheta = \Phi = 0$,

[‡]Here, we mean the usual parametrisation $\pi_1 \equiv |\vec{\pi}|\sin\vartheta\cos\varphi$, $\pi_2 \equiv |\vec{\pi}|\sin\vartheta\sin\varphi$, and $\pi_3 \equiv |\vec{\pi}|\cos\vartheta$, with $\varphi\,\epsilon\,[0, 2\pi)$ and $\vartheta\,\epsilon\,[0, \pi)$; and a similar one for the vector $\dot{\vec{\pi}}$.

and the 5 parameters needed for the initial condition are σ, $|\vec{\pi}|$, $\dot{\sigma}$, $|\dot{\vec{\pi}}|$ and Θ. We will only need the distribution of the three angles, φ, ϑ and Φ, to reconstruct the complete, 8-variable distributions of any physical quantity from the results for the ensemble of the 5-variable initial conditions.
The distribution (29) factorizes into three terms: a term depending on the fields and field derivatives, σ, $\dot{\sigma}$, $|\vec{\pi}|$ and $|\dot{\vec{\pi}}|$, a term depending on Θ, and a third term containing the other three angles, Φ, ϑ and φ. We may generate the first term using the rejection method introduced in the previous subsection. The second term can be obtained by transformation from a uniform deviate (see ref. [17]). This way, we can have a representative ensemble of the 5 parameters needed for the initial conditions. We can easily obtain the ensemble for the remaining three angles, for example, using the rejection method again. By forming pairs from the elements of the two ensembles, (let us define this operation as the product of the two ensembles) we have a representative ensemble of the original canonical distribution. However, we need to run the calculations only for the first ensemble in the product, while the second one we *apply* on the results as rotations. This enables us to choose the second ensemble as large as we wish. Furthermore, there are parameters, for example the neutral pion ratio, that we can calculate *analytically* by taking into account the distribution function of the second ensemble!
Let us show this in more detail. The joint distribution of the angles φ and ϑ is independent of the other variables in (29), moreover, it is the uniform distribution on the three-sphere, given by $\sin\vartheta\, d\vartheta\, d\varphi$. To reconstruct the distribution of the $\vec{\pi}$ field, we have to perform the rotations given by ϑ and φ on the states in the ensemble, which leads to a spherically symmetric π distribution at all proper times. Therefore, even though unlike ref. [10] we do *not* have an $O(4)$ isospin symmetry, for the neutral pion ratio, R, we obtain exactly the same distribution:

$$\mathcal{P}(R) = \frac{1}{2\sqrt{R}}.$$

C. Results for the ensemble of initial conditions

In this subsection we shall present the results of the generated ensembles of initial conditions. These ensembles depend on the freeze-out temperature and chemical potential, T_0 and μ_0, and on the volume of the DCC domain. The former two are determined since we start from a 20% supercooled baryon-free plasma, i.e., $T_0 = 130$MeV and $\mu_0 = 0$.
It is known [10] that at $T \approx T_c$ the correlation length in the linear sigma model is comparable to the pion size. To simulate these most probable initial domain sizes, we have chosen the value $V_0 = 0.5\text{fm}^3$.
To give a comparison to the Gaussian initial condition (23), we also tried $V_0 = 3.3\text{fm}^3$ since that gives exactly the same initial field derivative distributions.
Unfortunately, our model does not include the dynamical evolution of the domain sizes. It is not clear what the survival rates for domains of different sizes are and it may occur that relatively large domains have the best chance to survive. That is why we chose a third value, $V_0 = 10\text{fm}^3$, for our analysis.
All three initial ensembles contained 15,000 states.

1. Various distributions of the initial ensemble

a. The distribution of the chiral fields. Fig. 3 shows the joint distribution function[§] of the chiral field σ and the length of the isovector $\vec{\pi}$ in the initial ensemble. As we expected, the peak of the distribution is not at $\sigma = 0$, however it is not at the minimum ($\sigma \approx 40$MeV) of the potential energy density, either. This is because of the quarks. The quark energy density is a monotone decreasing function of $\sigma^2 + \vec{\pi}^2$, therefore it is more favourable energetically to have a larger condensate, ≈ 86MeV.
For bigger volumes the distributions are sharper. The reason is that fluctuations are smaller in larger systems. Thus, the probability for the system to be far from the minimum of the potential energy density is larger for small systems. This increases the probability of having large oscillations, which helps the observability of the domain. However, this increase may be compensated by the fact that small domains emit fewer pions. Unfortunately, our one-dimensional model does not allow us to decide this question because it includes only a scaling expansion of the domains but cannot account for domain evolution due to instabilities.
As a comparison, Fig. 2 shows the $\sigma - |\vec{\pi}|$ distribution for the microcanonical ensemble shown in Fig. 7 in ref. [1]. The states in the ensemble are concentrated in a circular band, which is rather different from our peaked distributions. This is a consequence of the high initial chiral "angular momentum" and the constraint that these initial states all have the same energy.
b. The distribution of the quark/antiquark effective mass. The initial distribution of the chiral fields implies that the initial quark mass is very unlikely to be zero, which

[§] These distributions were obtained by introducing a rectangular grid in the $\sigma - |\vec{\pi}|$ plane and counting the states in each grid cell with a $1/\vec{\pi}^2$ weight. The value of the distribution function in a given grid cell was approximated by the ratio of the total for the cell to the area of the cell. Then we divided by the total number of states to normalize the distributions to unity. Since the $1/\vec{\pi}^2$ Jacobian enhances statistical fluctuations for small $|\vec{\pi}|$ values tremendously, we had to take a huge ensemble of 600,000 states for these plots. These fluctuations also depend on the cellsize; the distributions are smoother for bigger cells. We have chosen a cellsize of 20MeV in both the σ and $|\vec{\pi}|$ direction.

again questions the appropriateness of the choice (20). The actual distribution** of the effective quark mass is shown in Fig. 4. As the initial volume decreases, the distribution broadens and the average quark/antiquark mass increases.

c. The distribution of the proper time derivatives of the fields. By Eqs. (21) and (22), the proper time derivatives of the chiral fields follow Gaussian distributions with the same width, $\sqrt{T_0/V_0}$. For a given freeze-out temperature, the width is *inversely* proportional to $\sqrt{V_0}$. In ref. [11] and followers [12,14,18,13] this width is assumed to be order of v, interpreted as $v/1$fm, which is 88MeV/fm. This is the same order of magnitude as our results and would correspond to $V_0 = 3.3\text{fm}^3$ at $T_0 = 130$MeV. To obtain a significantly lower width, one has to take an extremely low freeze-out temperature and/or a very large domain size.

d. The distribution of the quark, potential and kinetic energy densities. The distribution of the quark, potential and kinetic energy densities of the initial conditions can be seen in Figs. 5, 6, and 7. We can see that the kinetic, potential and quark energy densities have the same order of magnitude.

Due to the increasing fluctuations, all distributions spread as the initial volume decreases. Furthermore, the peaks of the kinetic and potential energy density distributions shift to higher values. This is in agreement with our picture: more fluctuations result in more kinetic energy density, and thus the system climbs higher and higher on the wall of the valley of the potential energy density. On the other hand, for the quarks the peak shifts to lower values for increasing initial volumes. This is due to the fact that fluctuations increase the quark/antiquark effective mass.

The distribution of the kinetic energy density (22) can be calculated analytically. Using that $\mathcal{H}_{kin} = \dot{\vec{\Phi}}^2/2$, from Eq. (29) it is not difficult to obtain that

$$f(\mathcal{H}_{kin})\, d\mathcal{H}_{kin} = \left(\frac{V_0}{T_0}\right)^2 \exp\left(-\frac{V_0}{T_0}\mathcal{H}_{kin}\right) \mathcal{H}_{kin}\, d\mathcal{H}_{kin} \ .$$

A simple calculation yields that the maximum of the initial kinetic energy distribution is at $\mathcal{H}_{kin} = T_0/V_0$. This value is $2-3$ orders of magnitude larger than the kinetic energy density corresponding to the initial condition (20), which is about 0.066MeV/fm^3.

2. The evolution of the ensemble

a. The evolution of the ensemble of the chiral fields. Figs. 8 and 9 show the time evolution of the ensemble average and the 70% fraction of the chiral fields, σ and π_1, for freeze-out times $\tau_0 = 1\text{fm}/c$ and $7\text{fm}/c$. The other two pion fields, π_2 and π_3, have a similar evolution to that of π_1 because of the rotational symmetry.

Here, by average we mean the arithmetic mean, while the "70% fraction" is the interval that is centered on the average and contains 70% of the ensemble. One could also use the usual estimate of the standard deviation but, because the distributions are non-Gaussian, that would not correspond to the same fraction of the ensemble at different proper times (we determined that in our case one standard deviation means an at least 60% fraction, while two standard deviations correspond to at least 90%).

The 70% fraction helps us pick out very unlucky events, i.e., those which are very far out of the interval. These intervals are narrower for bigger systems, due to the well-known fact that fluctuations are smaller in bigger systems [19–21].

The time evolution from the initial condition (20) with $\tau_0 = 1\text{fm}/c$ is rather uncharacteristic for the majority, at least 90%, of the ensemble, as from time to time the σ field is away from the average by about two standard deviations. For $\tau_0 = 7\text{fm}/c$ the situation is slightly better - the above fraction is 80%. This is because the damping is reduced due to the slower expansion, therefore the distribution becomes wider. We conclude, that the initial condition (20) is representative only if the initial ensemble has larger fluctuations, i.e., we have a much higher initial temperature or smaller initial volume, which is physically unreasonable.

However, the evolution of the pion fields is well in the 70% fraction. Thus, the initial condition (20) does *not* overestimate pion oscillations. Furthermore, due to the small starting kinetic energy, the oscillations are deep in the 70% interval, showing that oscillations with larger amplitudes would be similarly probable. The oscillations are out of the 70% fraction only if the initial ensemble contains little fluctuations, i.e., if the initial temperature is very low and/or the initial volume is very large.

Figs. (8) and (9) also tell that the Gaussian initial condition (23) results in a very similar ensemble evolution to that for $V_0 = 3.3\text{fm}^3$ and $T_0 = 130$MeV. The 70% intervals are almost identical, showing that both ensembles are concentrated in the same regions. The mean values are identically zero for the π_1 distribution as a consequence of the rotational symmetry. However, the σ means are quite different because the distributions have different shapes and the initial distribution (23) is peaked at $\sigma = 0$, which is not the correct value of the condensate at $T_0 = 130$MeV.

** All one-dimensional distributions were calculated by dividing the plotted interval into $40 - 50$ equal sections and counting the number of states in each section. All these distributions are normalized to unity.

VI. CONCLUSIONS

In this work we investigated chiral condensate evolution starting from a canonical ensemble of initial states. In the scenario we presented, the initial ensemble and its subsequent evolution is characterized by three simple parameters: the freeze-out temperature, T_0, the initial volume, V_0, and the freeze-out time τ_0.

We compared our initial condition to the "roll-down" scenario, i.e., to starting from the unstable maximum of the potential with a little kick [14,15,9]. We found that the sigma field evolution in the "roll-down" scenario is unrealistic because the sigma field oscillates counterphase, however pion oscillations are not overestimated if we choose reasonable values for the parameters, i.e., if $T_0 = 130\text{MeV}$, $V_0 \sim 0.5 - 10\text{fm}^3$, and $\tau_0 \sim 1 - 7\text{fm}/c$. Thus we confirm the suggestions [22] and the findings [16] that observable DCC is a rare event in a canonical ensemble.

We also made a comparison to the often-quoted Gaussian field and field derivative distributions with widths v and $v/1\text{fm}$ respectively [11,12,14,18]. We found that these distributions are quite close to the choice $T_0 = 130\text{MeV}$ and $V_0 = 3.3\text{fm}^3$. However, this choice also accounts for the necessary non-zero mean of the σ distribution corresponding to the non-zero condensate at a finite temperature, $T_0 \sim 130\text{MeV}$.

We believe that our simple scenario gives more insight on what the proper initial conditions could be. Though our results are similar to those obtained from other initial conditions, the ones mentioned above and their modifications [13], we did contribute to reducing the arbitrariness in those. Our three parameters have clear physical meaning, and they give a simple way and a good handle on how to choose the initial field distributions.

One should keep in mind that all our calculations were done in a one-dimensional Bjorken scaling picture. To obtain quantitative answers on domain sizes one inevitably has to take into account the spatial dimensions as well. Our test calculations based on the linear response method indicate that the fastest growth rates are about $1c/\text{fm}$, thus the biggest domains are $3 - 4\text{fm}$ large. This is in agreement with earlier findings [12,14,13,3,15]. However, we would like to emphasize that the only way to make real quantitative statements about the observability of DCCs is to go one step further and calculate observables, e.g., to obtain the spectra of pions emitted by the domains.

ACKNOWLEDGEMENTS

Enlightening discussions with T. Biró and M. Gyulassy are gratefully acknowledged. This work was supported by the Research Council of Norway (through its programs for nuclear and particle physics, supercomputing and free projects), and by the Director, Office of Energy Research, Division of Nuclear Physics of the Office of High Energy and Nuclear Physics of the US Department of Energy under Contract Number DE-FG02-93ER40764.

[1] T.S. Biró, D. Molnár, Z. Feng, L.P. Csernai, *Phys. Rev.* **D55** (1997) 6900.
[2] T. Csörgő and L.P. Csernai, *Phys. Lett.* **B333** (1994) 494.
[3] L. P. Csernai and I.N. Mishustin, *Phys. Rev. Lett.* **74** (1995) 5005.
[4] J.D. Bjorken, *Phys. Rev.* **D27** (1983) 140.
[5] L.D. Landau and E.M. Lifshitz: *The Classical Theory of Fields* (Pergamon, 1962).
[6] L.P. Csernai: *Introduction to relativistic heavy ion collisions* (Wiley, 1994).
[7] J.I. Kapusta and A.M. Srivastava, *Phys. Rev.* **D50** (1994) 5379.
[8] S. Gavin and B. Müller, *Phys. Lett.* **B329** (1994) 486.
[9] Z. Feng, D. Molnár and L.P. Csernai, *Heavy Ion Phys.* **5** (1997) 127.
[10] K. Rajagopal and F. Wilczek, *Nucl. Phys.* **B399** (1993) 395.
[11] K. Rajagopal and F. Wilczek, *Nucl. Phys.* **B404** (1993) 577.
[12] S. Gavin, A. Gocksch and R.D. Pisarski, *Phys. Rev. Lett.* **72** (1994) 2143.
[13] M. Asakawa, Z. Huang, and X.N. Wang, *Phys. Rev. Lett* **74** (1995) 3126.
[14] Z. Huang and X.-N. Wang, *Phys. Rev.* **D49** (1994) 4335.
[15] L.P. Csernai, T.S. Biró, Z.H. Feng, I.N. Mishustin, Á. Mócsy, D. Molnár and O. Scavenius, *Heavy Ion Phys.* **4** (1996) 45.
[16] T.S. Biró and C. Greiner, *Phys. Rev. Lett.* **79** (1997) 3138.; C. Greiner and B. Müller, *Phys. Rev.* **D55** (1997) 1026.
[17] W.H. Press, et al.: *Numerical recipes in C: the art of scientific computing* (Cambridge University Press, 1992 – 2nd edition).
[18] A. Bialas, W. Czyz and M. Gmyrek, *Phys. Rev.* **D51** (1995) 3739.
[19] K. Huang: *Statistical Mechanics* (Wiley, 1966).
[20] F. Reif: *Fundamentals of statistical and thermal physics* (McGraw-Hill, 1965).
[21] L.D. Landau and E.M. Lifshitz: *Statistical Physics* (Pergamon, 1959).
[22] J.-P. Blaizot and A. Krzywicki, *Acta Phys. Pol.* **B27** (1996) 1687.

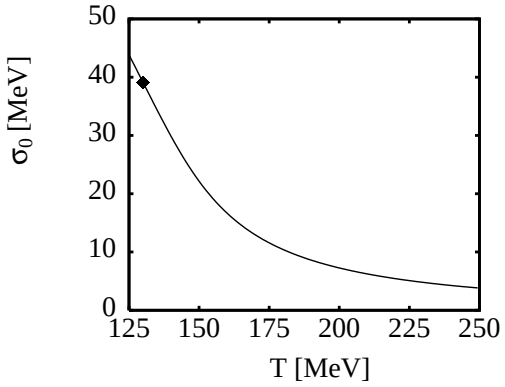

FIG. 1. The minimum of the potential energy density as a function of the temperature with our standard model parameters. Clearly, the condensate is non-zero even at high temperatures. The 'diamond' indicates its value at the freeze-out temperature $T_0 = 130$MeV.

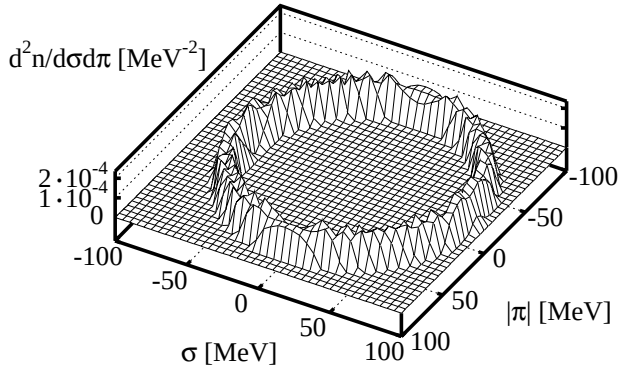

FIG. 2. The initial distribution of the chiral field σ and the magnitude of the isovector $\vec{\pi}$, for the microcanonical distribution in Fig. 7 in ref. [1]. Unlike the peaked canonical distributions in Fig. 3, the states are concentrated in a circular band. The initial ensemble contained 600,000 states and, to aid the eye, the distribution was complemented by a reflection on the $|\vec{\pi}| = 0$ plane.

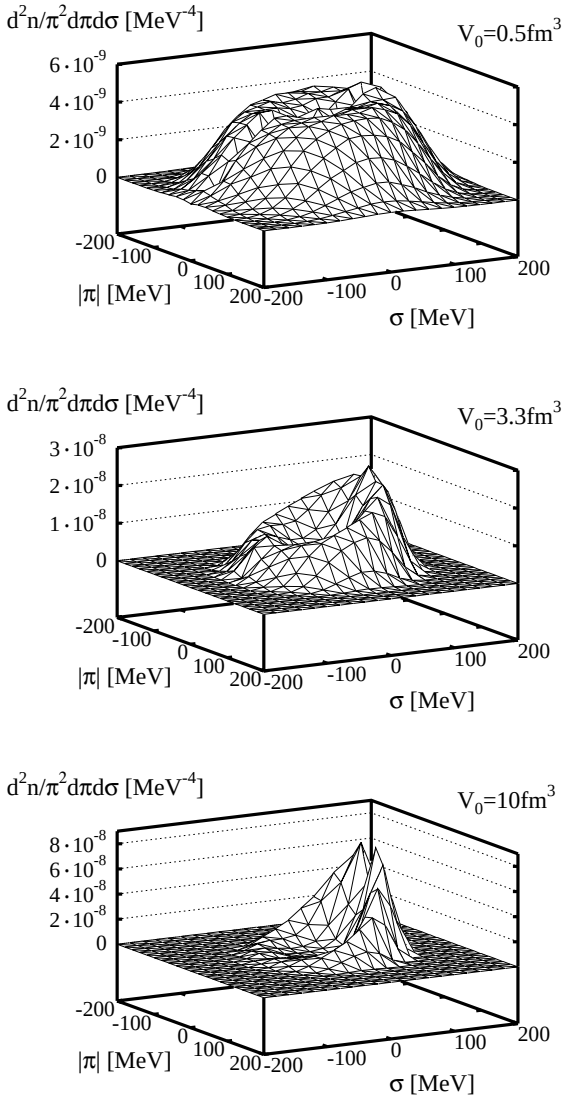

FIG. 3. The initial distribution of the chiral field σ and the magnitude of $\vec{\pi}$, for initial volumes $V_0 = 0.5\text{fm}^3$ (top), 3.3fm^3 (middle) and 10fm^3 (bottom), at the initial temperature $T_0 = 130$MeV for an ensemble of 600,000 states. Manifestly, the distribution has its maximum at a non-zero σ value and becomes narrower for a larger initial volume. To aid the eye, the distributions were complemented by a reflection on the $|\vec{\pi}| = 0$ plane.

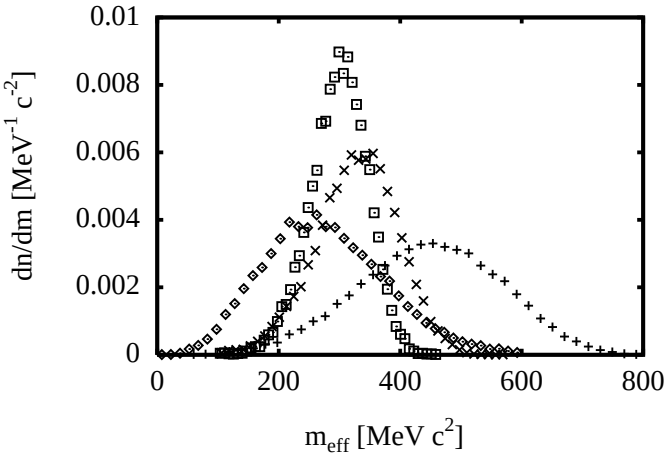

FIG. 4. The initial distribution of the effective quark/antiquark mass for initial volumes $V_0 = 0.5\text{fm}^3$ (pluses), 3.3fm^3 (crosses) and 10fm^3 (boxes), at the initial temperature $T_0 = 130\text{MeV}$ for an ensemble of 15,000 states. The 'diamonds' correspond to the Gaussian initial condition (23). As the initial volume decreases, mass fluctuations intensify and the average mass increases.

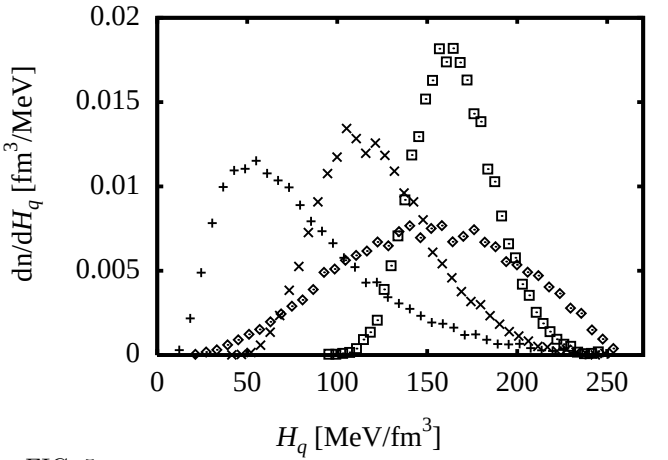

FIG. 5. The initial distribution of the quark energy density density (22) for initial volumes $V_0 = 0.5\text{fm}^3$ (pluses), 3.3fm^3 (crosses) and 10fm^3 (boxes), at the initial temperature $T_0 = 130\text{MeV}$ for an ensemble of 15,000 states. The 'diamonds' correspond to the Gaussian initial condition (23). Since for smaller initial volumes the quark mass tends to be bigger, the quark energy density is then smaller.

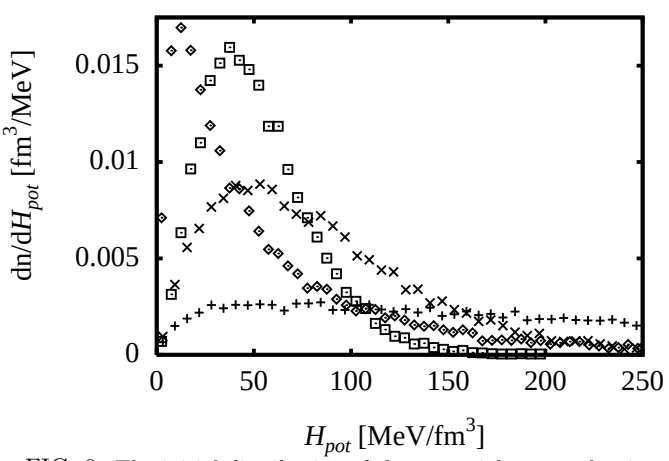

FIG. 6. The initial distribution of the potential energy density (22) of the meson fields for initial volumes $V_0 = 0.5\text{fm}^3$ (pluses), 3.3fm^3 (crosses) and 10fm^3 (boxes), at the initial temperature $T_0 = 130\text{MeV}$ for an ensemble of 15,000 states. The 'diamonds' correspond to the Gaussian initial condition (23). As the initial volume decreases, the system is more and more probable to be on the walls of the valley of the potential energy density, far from the minimum.

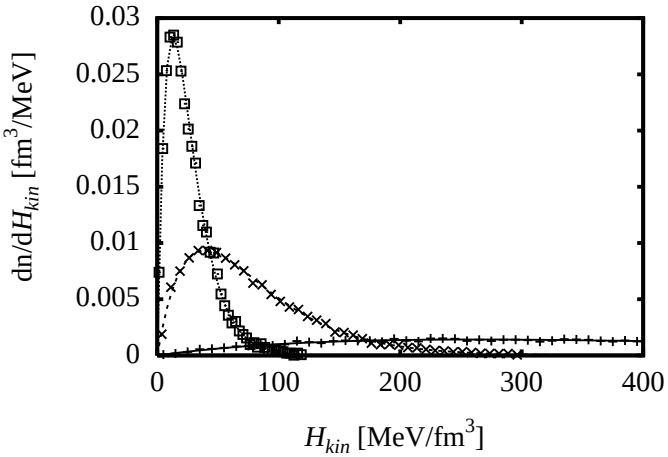

FIG. 7. The initial distribution of the kinetic energy density (22) of the meson fields for initial volumes $V_0 = 0.5\text{fm}^3$ (pluses), 3.3fm^3 (crosses) and 10fm^3 (boxes), at the initial temperature $T_0 = 130\text{MeV}$ for an ensemble of 15,000 states. The distribution for the Gaussian initial condition (23) is identical to taking $V_0 = 3.3\text{fm}^3$. The agreement with the theoretical curves is excellent. For smaller initial volumes fluctuations are larger, and thus the kinetic energy distribution is broader and the average kinetic energy density is larger.

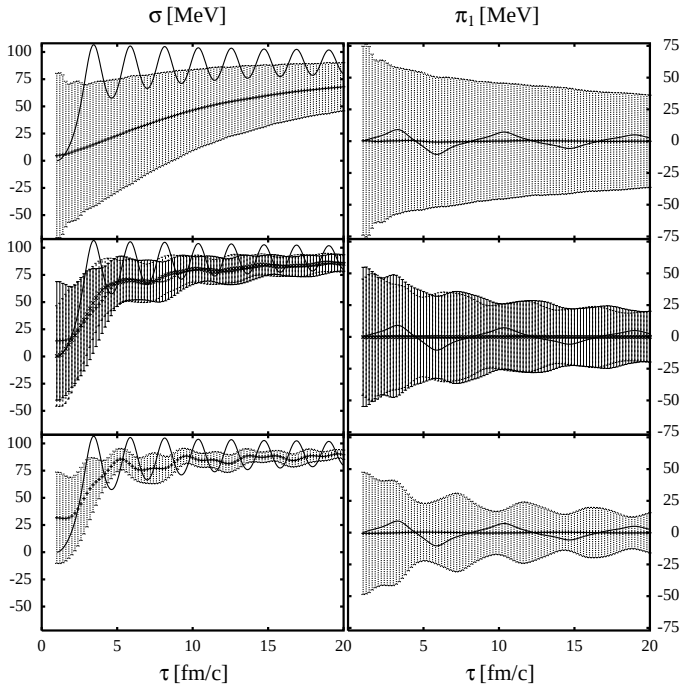

FIG. 8. The time evolution of the ensemble average and "70% interval" of the σ and π_1 fields for initial volumes $V_0 = 0.5\text{fm}^3$ (top), 3.3fm^3 (middle) and 10fm^3 (bottom), with a freeze-out time $\tau_0 = 1\text{fm}/c$, initial temperature $T_0 = 130\text{MeV}$, for an ensemble of 15,000. The shaded regions represent the 70% fraction centered on the mean value. The thin solid lines correspond to the evolution starting from the initial condition (20). The evolution of the σ field is rather uncharacteristic for the majority of the ensemble, showing that this initial condition is improbable. However, the oscillations of the pion fields are well within range, which is due to the rather small kinetic energy corresponding to (20). The middle figures also show the ensemble evolution for the Gaussian initial condition (23); mean values – crosses, 70% interval – dashed. The evolution is close to that from $V_0 = 3.3\text{fm}^3$.

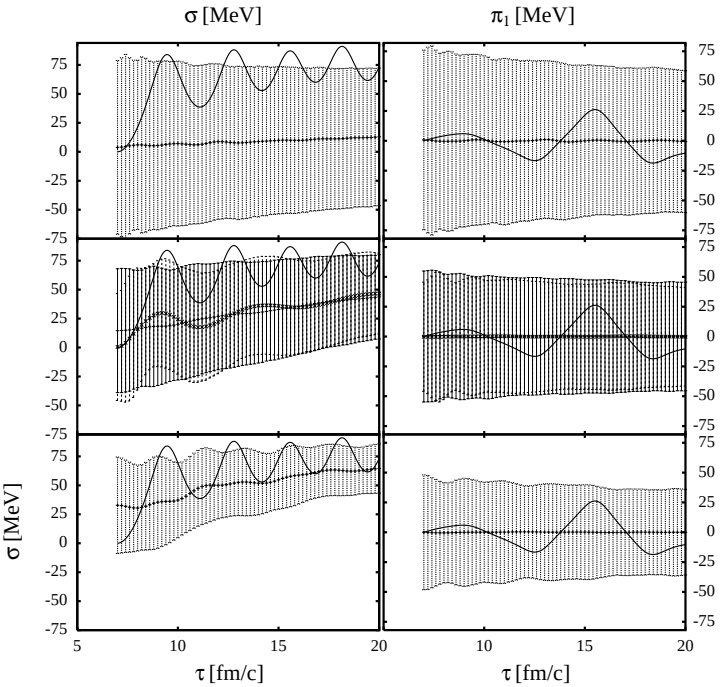

FIG. 9. The time evolution of the ensemble average and "70% interval" of the σ and π_1 fields for initial volumes $V_0 = 0.5\text{fm}^3$ (top), 3.3fm^3 (middle) and 10fm^3 (bottom), with a freeze-out time $\tau_0 = 1\text{fm}/c$, initial temperature $T_0 = 130\text{MeV}$, for an ensemble of 15,000. The shaded regions represent the 70% fraction centered on the mean value. The thin solid lines correspond to the evolution starting from the initial condition (20). The evolution of the σ field starting from the initial condition (20) is still uncharacteristic for the majority of the ensemble. However, the oscillations of the pion fields are well within range, which is due to the rather small kinetic energy corresponding to (20). The bottom figures also show the ensemble evolution for the Gaussian initial condition (23); mean values – crosses, 70% interval – dashed. The evolution is close to that from $V_0 = 3.3\text{fm}^3$.